

Mital Festschrift, pp. 181-197
W. J. Van Ooij and H. R. Anderson, Jr. (Eds)
© VSP 1998.

182

where a is
the micros

A new approach for determining roughness by means of contact angles on solids

R. J. GOOD,* M. K. CHAUDHURY† and C. YEUNG‡

Department of Chemical Engineering, State University of NY at Buffalo, Buffalo, NY 14260, USA

Abstract—Contact angle hysteresis on rough surfaces is caused by the contortion of the liquid surface that must occur as the liquid front passes from one metastable configuration to another. We have combined the Wenzel equation for the effect of roughness on the contact angle, θ , with the well-known equation relating contact angles to the surface free energy of the solid and of the liquid, and with Good's hypothesis of a free energy barrier to liquid front motion. The method that is developed calls for measuring θ for a series of liquids and plotting $\cos \theta_a$ vs. $\sqrt{\gamma_l^{LW}}/\gamma_l$ and extrapolating to the limit of $(1/\gamma_l) \rightarrow 0$. On a perfectly smooth, homogeneous surface, the intercept is -1 and the Wenzel ratio for a rough surface is given, approximately, by the negative of the value of the intercept. A shift of the γ_c value for the solid, due to roughness, is also predicted. Experimental data are presented for measurements with Teflon FEP.

Keywords: Contact angle hysteresis; roughness; Teflon FEP; Wenzel ratio.

1. INTRODUCTION

Surface roughness is one of the major causes of contact angle hysteresis [1]. The contact angle of a liquid on a solid is strongly affected by any deviations of the surface from ideality [2, 3], such as roughness. For a rigid, chemically homogeneous surface, Young's equation,

$$\gamma_{sv} - \gamma_{sl} = \gamma_{lv} \cos \theta_Y \quad (1)$$

can be exact only if the surface is smooth[§]. Wenzel [4] identified a roughness ratio, r ,

$$r = \frac{a}{A} \quad (2)$$

*To whom correspondence should be addressed.

†Present address: Department of Chemical Engineering, Lehigh University, Bethlehem, PA 18015, USA.

‡Present address: Department of Chemical Engineering, University of Illinois, Urbana, IL 61801, USA.

§Strictly speaking, a rough surface cannot be perfectly homogeneous as regards local energy density. So the theory that we employ must be recognized as an approximation for real surfaces.

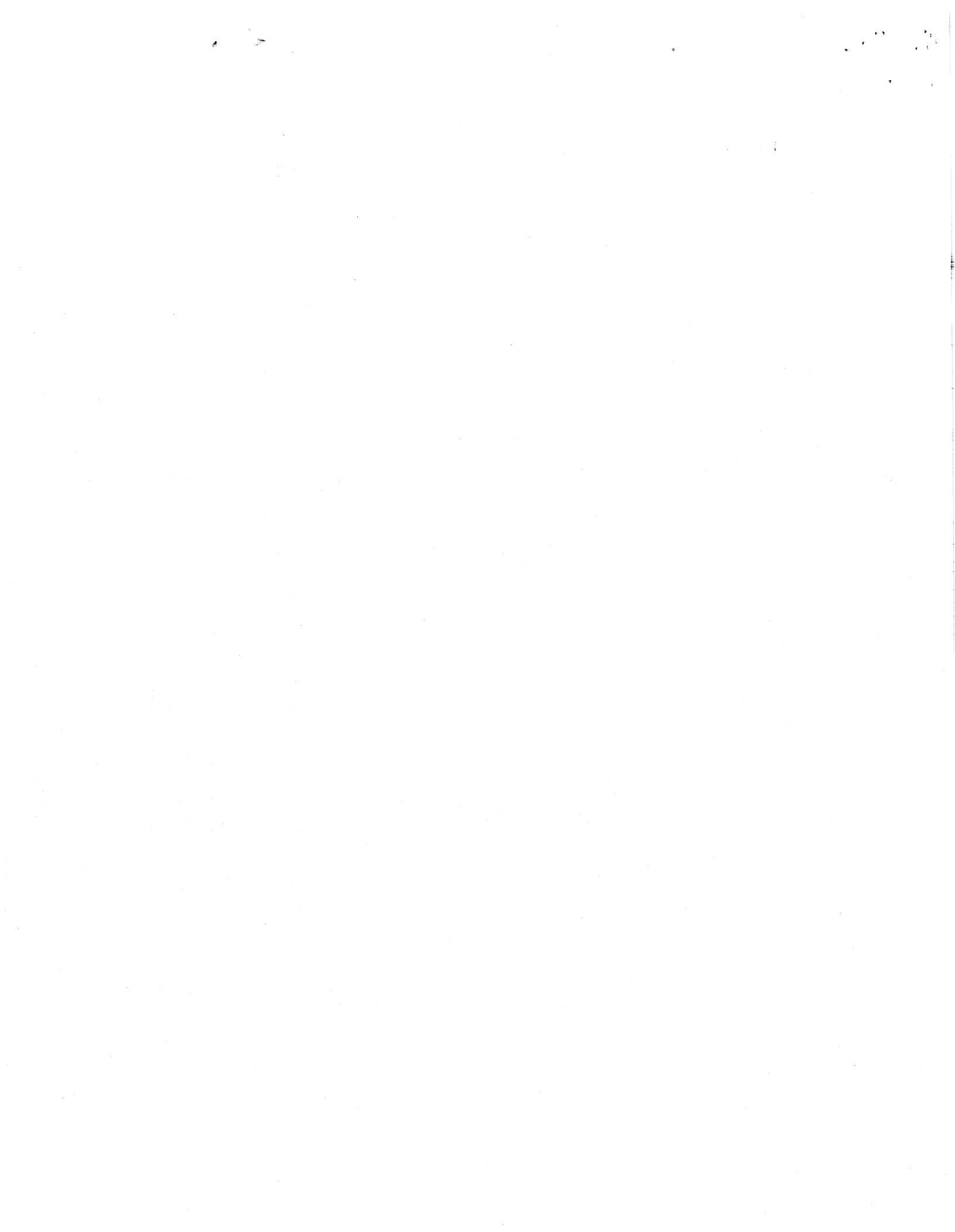
where θ_w
It has be
following :

where the
the surface
designated
polypropyl

Fox and Z
extrapolati
the critical
out that a p
extrapolati
mathematic
vs. $1/\sqrt{\gamma_l}$.

On the b
including
approach

Then in the
the point



where a is the actual, microscopic area and A is the apparent area, the projection of the microscopic area on a plane. The Young–Wenzel equation is

$$\cos \theta_W = \frac{r(\gamma_{sv} - \gamma_{sl})}{\gamma_l} \quad (3a)$$

$$= r \cos \theta_Y, \quad (3b)$$

where θ_W is the contact angle on the solid whose roughness ratio is r .

It has been shown [5–8] that for a liquid on a homogeneous smooth solid, the following general equation holds:

$$\gamma_l(1 + \cos \theta_Y) = 2\sqrt{\gamma_s^{LW}\gamma_l^{LW}} - 2\left(\sqrt{\gamma_s^\oplus\gamma_l^\ominus} + \sqrt{\gamma_s^\ominus\gamma_l^\oplus}\right), \quad (4a)$$

where the superscript LW denotes the apolar (London–van der Waals) component of the surface free energy [3, 8] and the polar (acid–base) components of γ_s and γ_l are designated by \oplus for Lewis acidity and \ominus for Lewis basicity. For apolar solids such as polypropylene and Teflon, γ_s^\oplus and γ_s^\ominus are zero, so that

$$\gamma_l(1 + \cos \theta_Y) = 2\sqrt{\gamma_s^{LW}\gamma_l^{LW}} \quad \text{if } \gamma_s^\oplus = \gamma_s^\ominus = 0 \quad (4b)$$

$$\cos \theta_Y = -1 + 2\sqrt{\gamma_s^{LW}} \left(\frac{\sqrt{\gamma_l^{LW}}}{\gamma_l} \right). \quad (4c)$$

Fox and Zisman [9] recommended plotting $\cos \theta$ vs. γ_l for a series of liquids, and extrapolating to the intercept with the line for $\cos \theta = 1$ ($\theta = 0$) to determine γ_c , the critical surface tension for the wetting of a solid. Good and Girifalco pointed out that a plot of $\cos \theta$ vs. $1/\sqrt{\gamma_l}$ gave a theory-based straight line, and hence (when extrapolation was required) a much more valid number for γ_c . Good [11] demonstrated mathematically the relation between the Fox and Zisman plot and the plot of $\cos \theta$ vs. $1/\sqrt{\gamma_l}$.

On the basis of the form of equations (4b) and (4c), Fowkes [10a, b] recommended including a point at ($\gamma_l^{-1} = 0, \cos \theta = -1$) in a plot of $\cos \theta$ vs. $\sqrt{\gamma_l^{LW}}/\gamma_l$. This approach needs to be improved upon, by combining equations (4c) and (3b):

$$\cos \theta_W = -r + 2r\sqrt{\gamma_s^{LW}} \left(\frac{\sqrt{\gamma_l^{LW}}}{\gamma_l} \right). \quad (5)$$

Then in the graph of $\cos \theta$ vs. $\sqrt{\gamma_l^{LW}}/\gamma_l$ the line should *not* be forced to go through the point (0, -1). The intercept at $\gamma_l^{-1} \rightarrow 0$ should be a measure of the roughness.

We will show below how the extrapolation of the observed advancing and retreating $\cos \theta$ values can be used to obtain a measure of the Wenzel roughness ratio.

The critical surface tension for wetting, γ_c , should also be a function of the roughness. From equations (3) and (5), with $\cos \theta = 1$,

$$\gamma_c^{LW} = \gamma_s^{LW} \left(\frac{2r}{1+r} \right)^2, \tag{6}$$

provided that (as is commonly the case) the critical wetting liquid is apolar. If the true value of γ_s^{LW} has been determined, using a molecularly smooth sample, then for a rough sample an *apparent* critical surface tension, γ_c^* , may be determined using the contact angle of a series of liquids. The roughness may be obtained by means of equation (7), which is equation (5) for $\theta_w = 0$:

$$r = \left[-1 + 2\sqrt{\gamma_s^{LW} \left(\frac{\sqrt{\gamma_c^{LW*}}}{\gamma_l} \right)} \right]^{-1}. \tag{7}$$

2. HYSTERESIS THEORY

In 1952 [1], it was proposed that hysteresis on a chemically homogeneous, rigid solid could be explained as due to the free energy of activation, F_a or F_r , required in order for a liquid front to move from one metastable configuration to another while a constant *local* angle at the solid surface is maintained. Equation (8) is a slightly modified form of the equation in ref. [1]:

$$\gamma_l \cos \theta_a = r(\gamma_s - \gamma_{sl}) - F_a \tag{8a}$$

$$\gamma_l \cos \theta_r = r(\gamma_s - \gamma_{sl}) - F_r \tag{8b}$$

Figure 1 shows a model surface with a sinusoidal cross-section, and indicates the location of the liquid front such that the local angle is the Young angle and the shape of the liquid surface (e.g. for a drop whose volume is constant) is determined by the constancy of the Laplace curvature ($1/\rho_1 + 1/\rho_2$), where the ρ 's are principal radii of curvature, over the whole liquid surface. When the drop front is not at a (metastable) equilibrium location, the curvature must depart from constancy, and this will cost energy, e.g. F_a .

Johnson and Dettre [12] used a model of a surface having ridges in concentric rings, with a sinusoidal profile. A drop of liquid is placed at the center, and liquid is added or withdrawn so that the diameter changes slowly. The free energy of activation is due to the local increase (or decrease) in area of the liquid surface. Consider the liquid to be a drop whose volume is constant. If the liquid surface is a section of a sphere when the front is in a metastable configuration, then a small motion (say,



Figure 1. (a) A model location, to the left of

from right to left) returning to a minimum.

If, instead of constant curvature, the liquid surface is in a metastable state, the local angle is being minimized together with volume.

The magnitude of the liquid, as hypothesized that

It should not be from the experiment, F_r , must be more

Then equations (8)

The Wenzel angle, θ_w , retreating angle, θ_r , combined with eq.

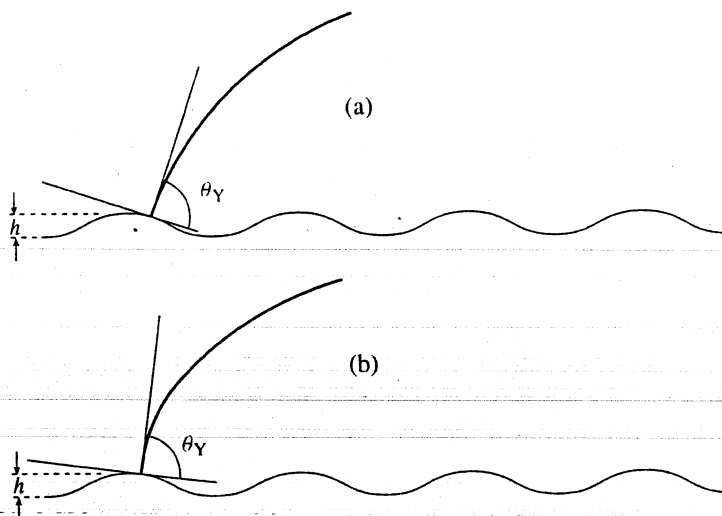


Figure 1. (a) A model surface with a liquid front at a metastable location. (b) Liquid front at an unstable location, to the left of the location in (a). Note the smaller radius of curvature near the solid.

from right to left) will require that the liquid/vapor area increase (or decrease) before returning to a minimized area when a new metastable configuration is reached.

If, instead of concentric rings, the surface consists of random hills and valleys, then in a metastable state the liquid front will wander across the surface in such a way as to keep the *local* contact angle as nearly constant as possible, with the free energy being minimized by allowing local contortion of the liquid surface near the solid, together with very local fluctuations of the contact angle away from the Young angle.

The magnitudes of the energy barriers should be a function of the surface tension of the liquid, as well as of the roughness ratio. For the advancing angle, we have hypothesized that

$$F_a = \gamma_l f_1(r). \quad (9a)$$

It should not be expected that F_r will be equal to F_a in general. It became evident from the experimental results that the form of the energy barrier in the retreating case, F_r , must be more complex than that of F_a . A possible form for F_r is

$$F_r = \gamma_l f_2(\gamma_l, r). \quad (9b)$$

Then equations (8a) and (8b) become

$$\gamma_l \cos \theta_a = r(\gamma_s - \gamma_{sl}) - \gamma_l f_1(r) \quad (10a)$$

$$\gamma_l \cos \theta_r = r(\gamma_s - \gamma_{sl}) - \gamma_l f_2(\gamma_l, r). \quad (10b)$$

The Wenzel angle is now taken, provisionally, to be the advancing angle, θ_a , or the retreating angle, θ_r , depending on the direction of the liquid front motion. Equation (8a) combined with equation (5) yields

$$\cos \theta_a = -r + r\sqrt{\gamma_s^{LW}} \left(\frac{\sqrt{\gamma_l^{LW}}}{\gamma_l} \right) - \gamma_l f_1(r) \quad (11a)$$

$$-r = \lim_{\frac{1}{\gamma_l} \rightarrow 0} [\cos \theta_a + f_1(r)] \quad (12a)$$

$$\gamma_c^{LW} = \gamma_s^{LW} \left(\frac{2}{1+r+f_1(r)} \right)^2 \quad (12b)$$

Also,

$$\cos \theta_r = -r + r\sqrt{\gamma_s^{LW}} \left(\frac{\sqrt{\gamma_l^{LW}}}{\gamma_l} \right) + \gamma_l f_2(\gamma_l, r) \quad (11b)$$

$$-r = \lim_{\frac{1}{\gamma_l} \rightarrow 0} [\cos \theta_r - f_2(\gamma_l, r)] \quad (12c)$$

$$\gamma_c^{LW} = \gamma_s^{LW} \left(\frac{2}{1+r+f_2(\gamma_l, r)} \right)^2 \quad (12d)$$

Thus, γ_c for a solid is a function of the roughness.

Now a data-handling method, for advancing angles, is to plot $\cos \theta_a$ vs. $\sqrt{\gamma_l^{LW}}/\gamma_l$ and extrapolate the regression line to the limit at the line, $\sqrt{\gamma_l^{LW}}/\gamma_l \rightarrow 0$. If the intercept is less than -1 , denote it by r^* :

$$r = r^* - f_1(r), \quad (13)$$

$$f_1(r) = -\cos \theta_a - r + 2r\sqrt{\gamma_s^{LW}} \left(\frac{\sqrt{\gamma_l^{LW}}}{\gamma_l} \right). \quad (14)$$

For this purpose, the value of γ_s^{LW} is needed. It can be determined using a sample of the solid that is actually smooth, with an apolar liquid such as CH_2I_2 , and the following equation [based on equation (4)]:

$$\gamma_s^{LW} \cong \frac{\gamma_l^{LW} (1 + \cos \theta_a)^2}{4}. \quad (15)$$

If a graph of $\cos \theta_a$ vs. $\sqrt{\gamma_l^{LW}}/\gamma_l$ for the smoothest available sample has indicated appreciable (but not too serious) roughness, e.g. according to equations (11a) and (12a), ignoring $f_1(r)$, then a second approximation can be estimated using

In principle should yield the case. Finally, composite for the rel

and replac

3. EXPERIMENTAL

3.1. Materials

Teflon FEP, graphite, SiC paper, as received, tropic, metric grade, bromobenzene, Eastman, alumina, F. Chemical

The diaphragm shot in a d with activ

3.2. Equipment

A Ramé H a zoom le could be WV-CM1 onto the s a stainless 'drop', with retreating after stop slight but lower-visc be satisf

$$\gamma_s^{LW} = \gamma_l^{LW} \frac{[1 + \cos \theta_a + f_l(r)]^2}{4} \quad (16)$$

In principle, the same general data-handling method applied to retreating angles should yield the same value of r as the advancing angle data. This turned out not to be the case.

Finally, we can compare samples of a particular solid that have the same surface composition, using the smoothest available surface as a reference sample. We write for the relative roughness, R ,

$$R = \frac{\cos \theta_{\text{rough}}}{\cos \theta_{\text{ref}}} = \frac{r}{r_{\text{ref}}} \quad (17)$$

and replacing r by R in all the above equations. For the reference surface, $R_{\text{ref}} \equiv 1$.

3. EXPERIMENTAL

3.1. Materials

Teflon FEP sheet from DuPont was used as received (after rinsing with a light hydrocarbon) for the 'smooth' solid, and it was roughened by random abrasion with SiC paper of various grit sizes. Lucite PMMA sheet, also from DuPont, was used as received. The liquids employed were triply distilled water; formamide, 99% spectrophotometric grade, Aldrich Chemical Co.; ethylene glycol, > 99%, spectrophotometric grade, Aldrich Chemical Co.; diiodomethane, 99%, Aldrich Chemical Co.; bromobenzene, ACS certified grade, Fisher Scientific Co.; benzene, Spectro ACS grade, Eastman Chemical Co.; *n*-octane, > 99%, Aldrich Chemical Co.; activated alumina, Fisher Scientific Co.; and activated carbon, Darco G-60, 100 mesh, Aldrich Chemical Co.

The diiodomethane was purified with activated carbon and stored over pure copper shot in a darkened container. The rest of the organic liquids were purified by treatment with activated alumina.

3.2. Equipment

A Ramé Hart contact angle goniometer, model 100-00, modified by the insertion of a zoom lens (for control of magnification without loss of focus) was used. Images could be recorded with a system consisting of a Panasonic video monitor, model WV-CM110A, and a Mitsubishi video printer, model P71U. The drops were delivered onto the solid samples with a micrometer syringe, from Fisher Scientific Co., with a stainless steel needle. The needle tip was used to hold the liquid as a 'captive drop', with the needle well centered. In measuring the advancing angle θ_a and the retreating angle θ_r , it was observed (on examination at higher magnification) that after stopping the addition or withdrawal of liquid, the three-phase line continued in slight but detectable motion for as much as 1 min with ethylene glycol. With the lower-viscosity liquids, a wait of 30 s before recording a measurement appeared to be satisfactory.

4. RESULTS

Tables 1 and 2 show the measured contact angles on Teflon FEP. Figure 2 was part of an early series of measurements. The Teflon FEP was from a different sample from that used in the rest of the study. The figure shows the graph of $\cos \theta_a$ and $\cos \theta_r$ for liquids on Teflon FEP vs. $\sqrt{\gamma_l^{LW}}/\gamma_l$ for the smoothest Teflon that was available. The extrapolated value of $\cos \theta_a$, for abscissa = 0, was -1.05 . The extrapolated value of $\cos \theta_r$ was -0.7 . The latter value is clearly not equal to $\cos \theta_a$. The extrapolated γ_c is $19.0 \pm 3 \text{ mJ/m}^2$ based both on θ_a and θ_r .

Figure 3 shows the $\cos \theta_a$ results for 'smooth' Teflon FEP, second series of measurements.* The estimate of $\cos \theta$ for $1/\gamma_l = 0$ is 1.07 ± 0.15 , in excellent agreement with Fig. 2. The error band was set at 95% confidence limits. The estimate of γ_c is $18.7 \pm 3.0 \text{ mJ/m}^2$, in excellent agreement with the earlier work. Figures 4, 5, and 6 show the curves of $\cos \theta_a$ vs. $\sqrt{\gamma_l^{LW}}/\gamma_l$ for surfaces that had been roughened with 4000, 1000, and 600 grit papers, respectively.

Table 1.

Advancing contact angles (in degrees) of some liquids on the Teflon FEP surface roughened with SiC paper of various grit sizes

Liquid	Teflon FEP surface roughened with:			
	4000 grit	1000 grit	600 grit	
Water	118.6 ± 1.9	125.8 ± 2.3	140.4 ± 3.7	155.6 ± 4.0
Formamide	102.7 ± 1.7	103.9 ± 2.3	120.2 ± 3.6	133.7 ± 3.0
Ethylene glycol	94.9 ± 0.8	93.8 ± 2.7	115.8 ± 3.0	132.2 ± 2.9
Diiodomethane	80.9 ± 1.1	95.7 ± 1.5	105.0 ± 2.6	112.4 ± 2.4
Bromobenzene	70.2 ± 0.5	75.4 ± 2.4	72.2 ± 2.9	80.0 ± 1.6
Benzene	58.0 ± 3.3	52.7 ± 3.0	54.5 ± 1.5	59.8 ± 1.8
Octane	34.6 ± 0.4	34.4 ± 1.7	0.0	0.0

Table 2.

Receding contact angles (in degrees) of some liquids on the Teflon FEP surface roughened with SiC paper of various grit sizes

Liquid	Teflon FEP surface roughened with:			
	4000 grit	1000 grit	600 grit	
Water	105.2 ± 1.3	97.6 ± 1.0	93.8 ± 2.3	128.7 ± 3.7
Formamide	86.5 ± 0.3	74.8 ± 1.7	76.3 ± 3.5	56.6 ± 2.2
Ethylene glycol	79.8 ± 0.6	65.6 ± 1.1	45.0 ± 1.1	28.5 ± 5.9
Diiodomethane	78.8 ± 0.7	70.5 ± 2.3	45.9 ± 3.1	0.0
Bromobenzene	58.1 ± 1.3	48.0 ± 0.9	0.0	0.0
Benzene	46.4 ± 1.7	31.9 ± 3.4	0.0	0.0
Octane	19.6 ± 0.9	9.9 ± 0.5	0.0	0.0

*The first series was conducted by M. K. Chaudhry and the second series by C. Yeung.

Figure 2.

Figure 3.
to 95% co

2 was part of
sample from
and $\cos \theta_r$ for
available. The
ated value of
trapolated γ_c
ries of meas-
nt agreement
mate of γ_c is
es 4, 5, and 6
ughened with

ghened with SiC

500 grit

- 155.6 ± 4.0
- 133.7 ± 3.0
- 132.2 ± 2.9
- 112.4 ± 2.4
- 80.0 ± 1.6
- 59.8 ± 1.8
- 0.0

ghened with SiC

600 grit

- 128.7 ± 3.7
- 56.6 ± 2.2
- 28.5 ± 5.9
- 0.0
- 0.0
- 0.0
- 0.0

eng.

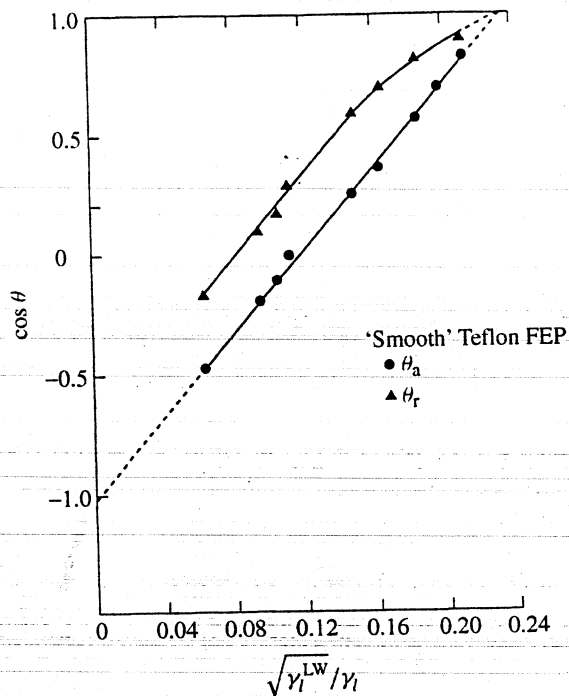


Figure 2. $\cos \theta_a$ and $\cos \theta_r$ for liquids on the 'smoothest' Teflon FEP, first series.

Advancing angles on 'smooth' Teflon FEP

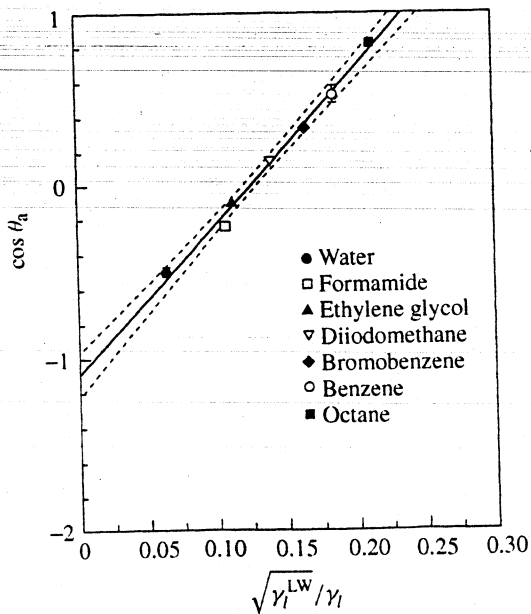


Figure 3. $\cos \theta_a$ for liquids on the 'smoothest' Teflon FEP, second series. The error band corresponds to 95% confidence limit.

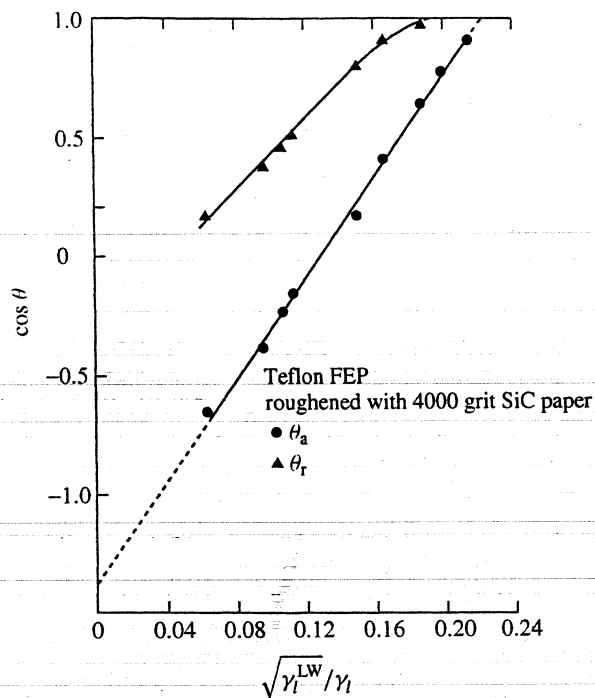


Figure 4. $\cos \theta_a$ and $\cos \theta_r$ for liquids on Teflon FEP roughened with 4000 grit SiC paper.

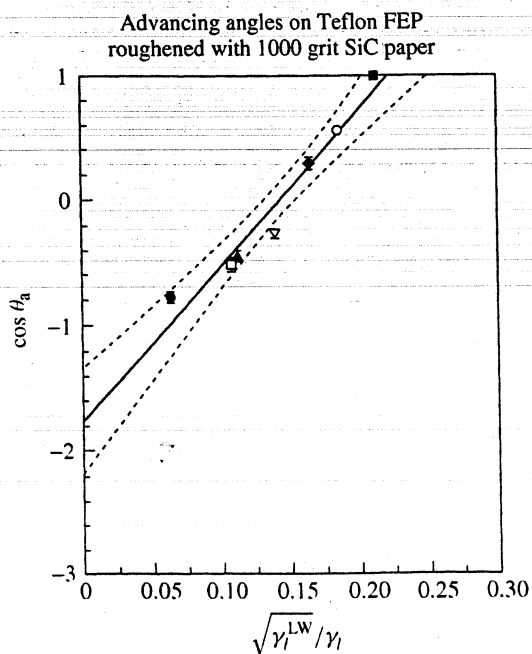


Figure 5. $\cos \theta_a$ for liquids on Teflon FEP roughened with 1000 grit SiC paper.

Figure 6.

Figure 7.

Figur
solid.
physic
the the

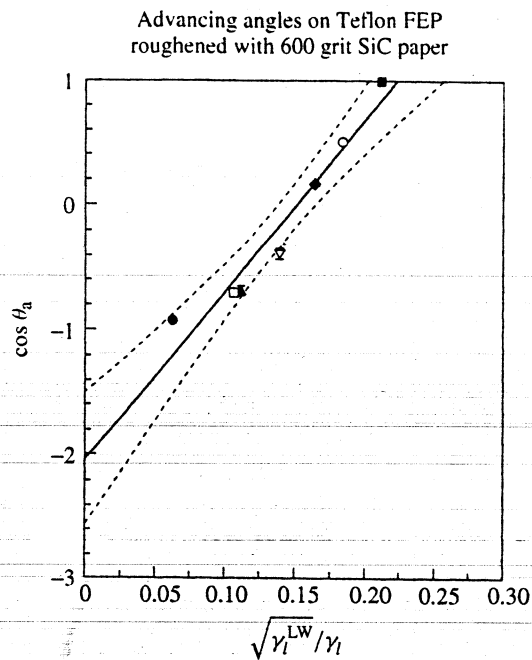


Figure 6. $\cos \theta_a$ for liquids on Teflon FEP roughened with 600 grit SiC paper.

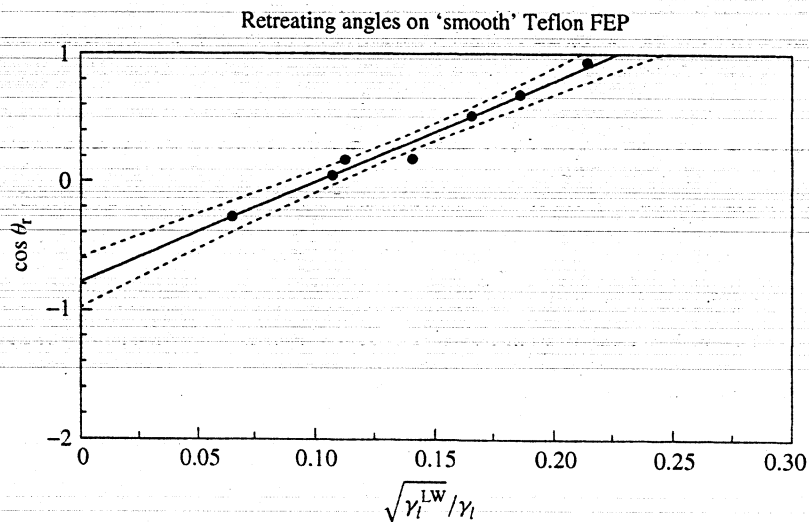


Figure 7. $\cos \theta_r$ for liquids on the 'smoothest' Teflon FEP.

Figures 7 and 8 show $\cos \theta_r$ for the smoothest Teflon and the 4000 grit-roughened solid. The $1/\gamma_l \rightarrow 0$ intercept is -0.8 ± 0.2 and -0.5 ± 0.3 , both of which are physically impossible as a measure of r . So we reach the tentative conclusion that the theory, i.e. equations (9)–(14), may not apply to retreating angles. This conclusion

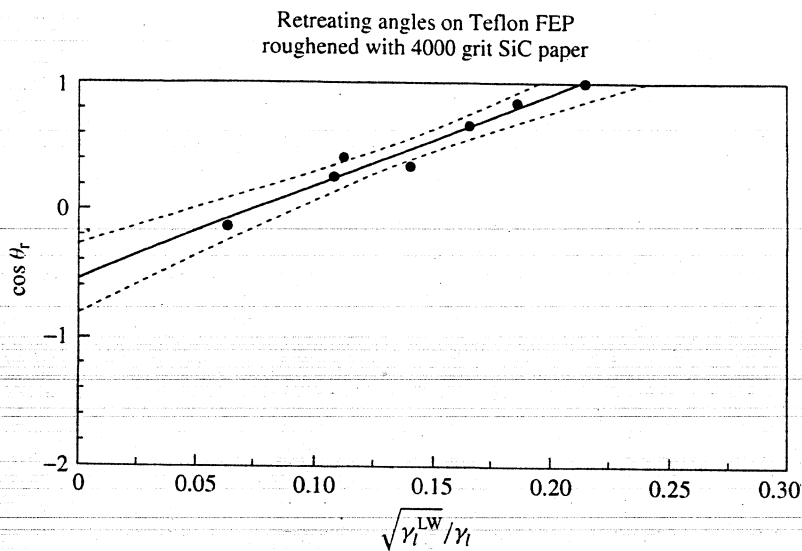


Figure 8. $\cos \theta_r$ for liquids on Teflon FEP roughened with 4000 grit SiC paper.

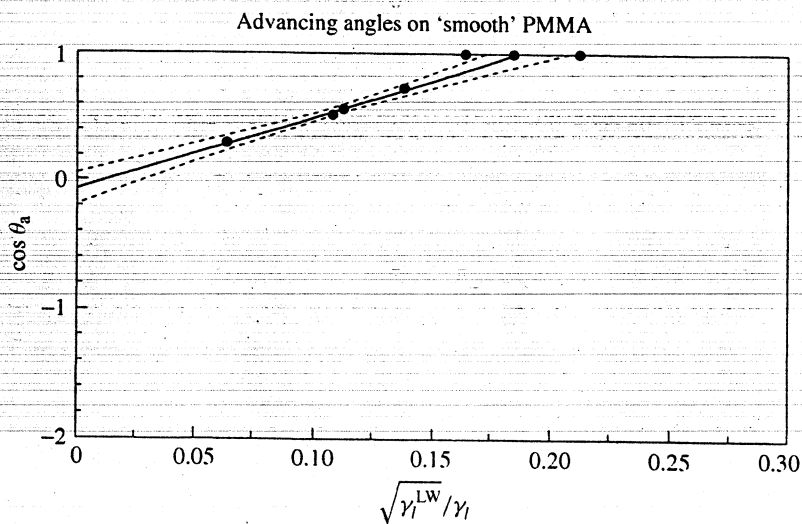


Figure 9. $\cos \theta_a$ for liquids on 'smooth' PMMA.

is supported by the fact that with retreating angles on Teflon FEP roughened with 1000 grit and 600 grit paper, γ_c was 37 mJ/m^2 on the former and 56 mJ/m^2 on the latter.

A series of θ_a measurements on roughened PMMA were also made (see Fig. 9 for the smoothest surface). The γ_c value was $37 \pm 10 \text{ mJ/m}^2$, in fair agreement with Zisman's value of 39 mJ/m^2 [13]. The intercept at $1/\gamma_l \rightarrow 0$ was at -0.1 ± 0.15 . For PMMA roughened on 4000 grit paper (Fig. 10), γ_c remained the same within experimental error, but the $\gamma^{-1} = 0$ intercept was -0.1 .

$\cos \theta_a$

Figure 10. c

θ_w

Figure 11. J

The compl
basic solid

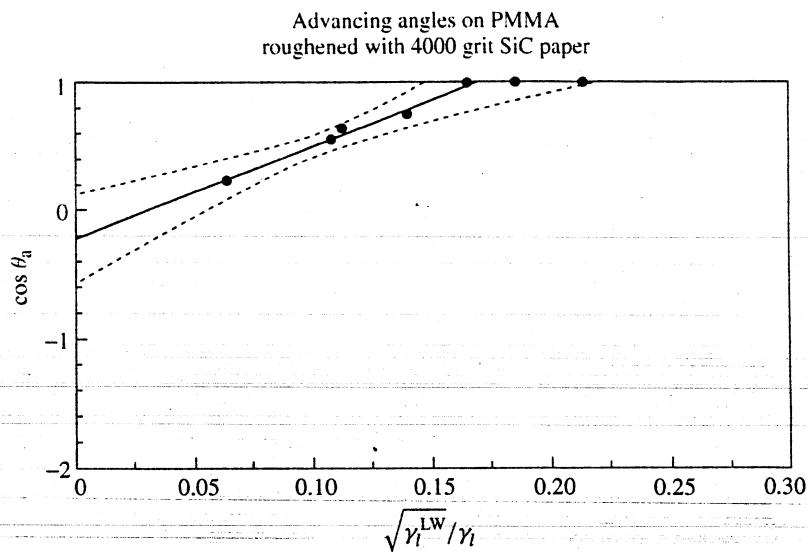


Figure 10. $\cos \theta_a$ for liquids on PMMA roughened with 4000 grit SiC paper.

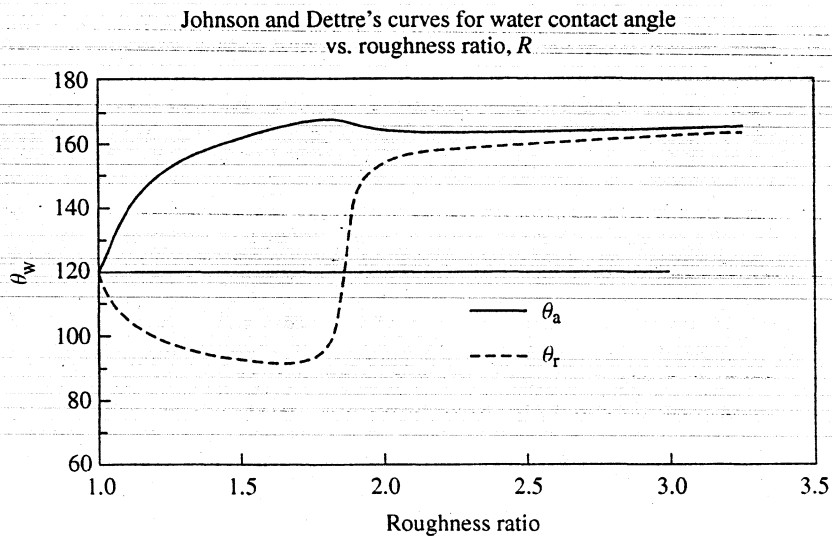


Figure 11. Johnson and Dettre's computations for the contact angle of water vs. the roughness ratio.

The combination of the Young–Wenzel equation with equation (4a) for a monopolar basic solid (such as PMMA) and a polar liquid is

$$\cos \theta_w = r \left[1 - 2\sqrt{\gamma_s^{LW}} \left(\frac{\sqrt{\gamma_l^{LW}}}{\gamma_l} \right) - 2\sqrt{\gamma_s^\ominus} \left(\frac{\sqrt{\gamma_l^\oplus}}{\gamma_l} \right) \right]. \quad (18)$$

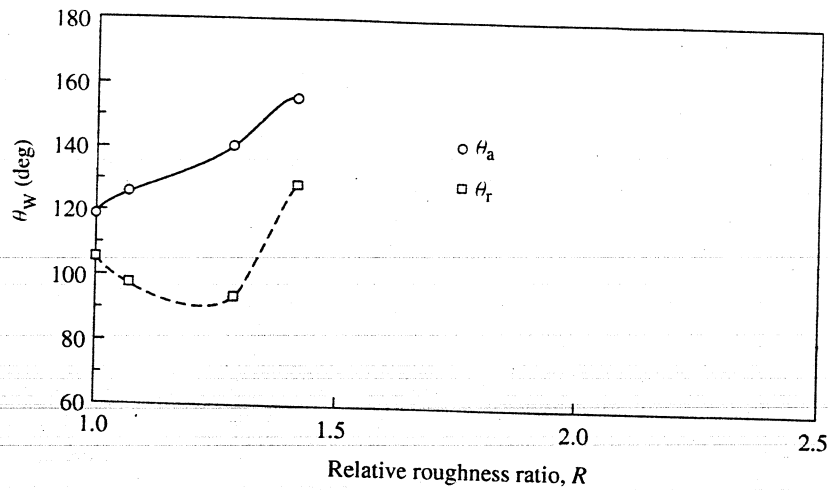


Figure 12. Observed contact angle of water on Teflon FEP vs. the relative roughness ratio R .

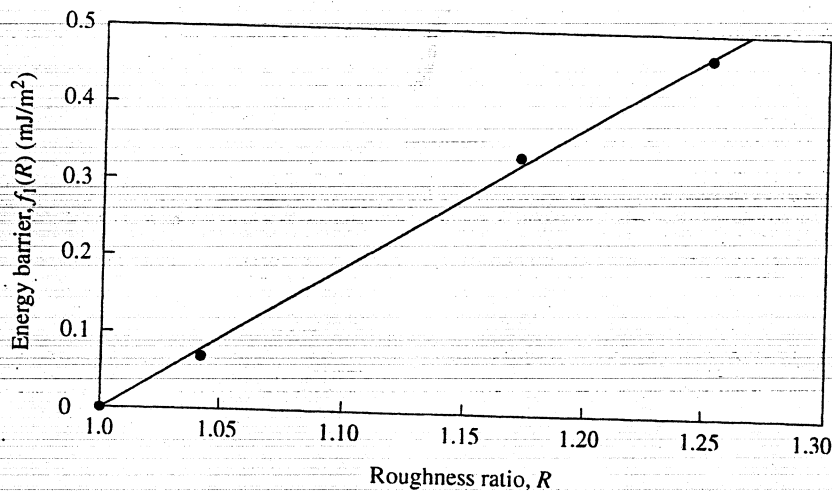


Figure 13. Energy barrier for liquid advance vs. the roughness ratio R on Teflon FEP.

It would not be expected, on the basis of equation (18), that the simple extrapolation of $\cos \theta$ vs. $\sqrt{\gamma_s^{LW}/\gamma_l}$ would yield very useful information.

Johnson and Dettre [12] computed the curve of advancing and retreating contact angles vs. the roughness ratio for their model surface (see Fig. 11). The sharp rise in $\cos \theta_r$, at about $r = 1.8$, was said to be due to the entrapment of air in the grooves on the surface. Our experimental results are shown in Fig. 12, which is in qualitative agreement with Fig. 11. The rise in $\cos \theta_r$, around $r = 1.4$, does correspond to the entrapment of air.

Table 3 shows the numerical results for roughened Teflon FEP. In this table, the value of 17.0 for γ_s^{LW} is probably valid because the roughness term ($r^* = 1.07$) is

Table 3. Results for r

Grit size
4000
1000
600

Figure 14. Sea

close to 1. T are less than with expectat

Figure 13 s

Table 3.
Results for roughened Teflon FEP

Grit size	Intercept r^*	γ_c^{LW} (mJ/m ²) (apparent)	γ_s^{LW} (mJ/m ²) (uncorrected)	R	$f_1(R)$ (mJ/m ²)
—	1.07 ± 0.15	17.6 ± 3	17.0	[1.0]	[0.0]
4000	1.23 ± 0.4	17.6 ± 4	15.7	1.07	0.070
1000	1.76 ± 0.6	19 ± 4	12.4	1.29	0.34
600	2.05 ± 0.75	21 ± 4	10.7	1.42	0.47



Figure 14. Scanning electron micrograph of 'smooth' Teflon FEP. Magnification $\times 500$.

close to 1. The apparent γ_c varies with the roughness. The values of γ_s^{LW} in column 4 are less than 17.0 mJ/m^2 , and do not represent the smooth solid. These trends agree with expectations.

Figure 13 shows the energy barrier, $f_1(R)$, as a function of R from our data.

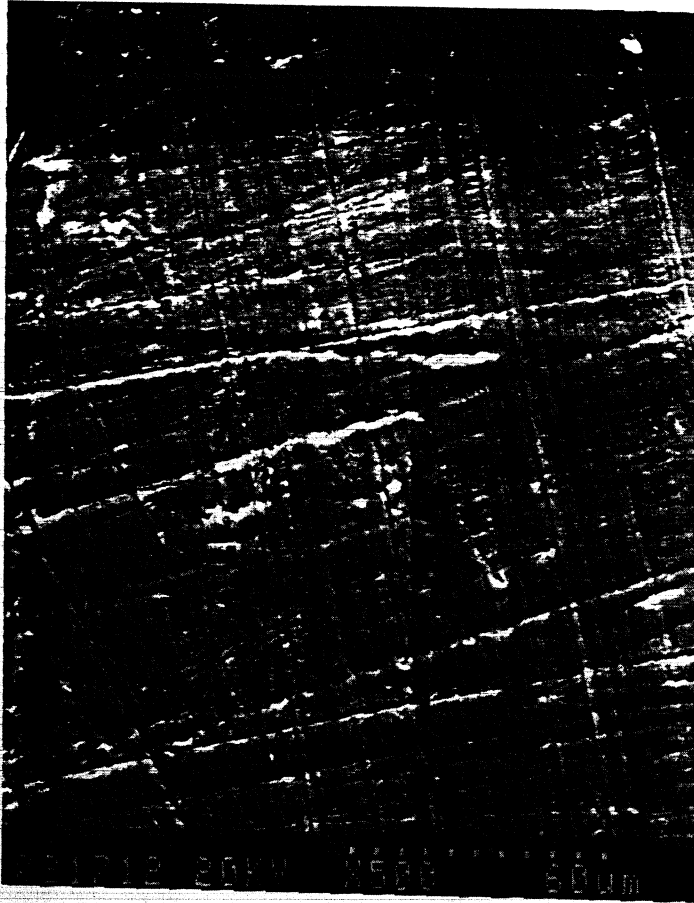


Figure 15. Scanning electron micrograph of Teflon FEP roughened with 4000 grit SiC paper.

We do not report the calculations based on the retreating angles. Values of r^* that were less than -1 indicated that the analysis was not applicable. We have not treated the data on PMMA, or other polar solids, for similar reasons.

Figures 14–16 show scanning electron micrographs of three of the surfaces that were studied.

5. CONCLUSIONS

We have developed and tested a method of determining the roughness of apolar solids from advancing contact angles. The method is validated for moderate roughness, e.g. up to a Wenzel roughness ratio of 1.4. The retreating angle, θ_r , appears to be less directly related to the Wenzel roughness than is θ_a . The energy barrier for liquid front advancing is about 0.5 mJ/m^2 for Teflon that has been abraded with 600 grit SiC paper.

Figure 16. Scanning electron micrograph of Teflon FEP roughened with 4000 grit SiC paper. Magnification $\times 500$.

Acknowledgements

We thank the General Motors Research Laboratories, Warren, Michigan, and the General Motors Industry/University Research Program, Buffalo for their support of this work. We also thank Dr. Charles A. J. Hoeve for his help in the early stages of this project.

REFERENCES

1. R. J. Good, *J. Polym. Sci. Polym. Chem. Ed.*, **10**, 1081 (1972).
2. R. J. Good, *J. Polym. Sci. Polym. Chem. Ed.*, **10**, 1085 (1972).
3. R. J. Good, *J. Polym. Sci. Polym. Chem. Ed.*, **10**, 1091 (1972).
4. (a) R. N. Young, *J. Polym. Sci. Polym. Chem. Ed.*, **10**, 1095 (1972).
(b) R. N. Young, *J. Polym. Sci. Polym. Chem. Ed.*, **10**, 1101 (1972).
5. R. J. Good, *J. Polym. Sci. Polym. Chem. Ed.*, **10**, 1107 (1972).

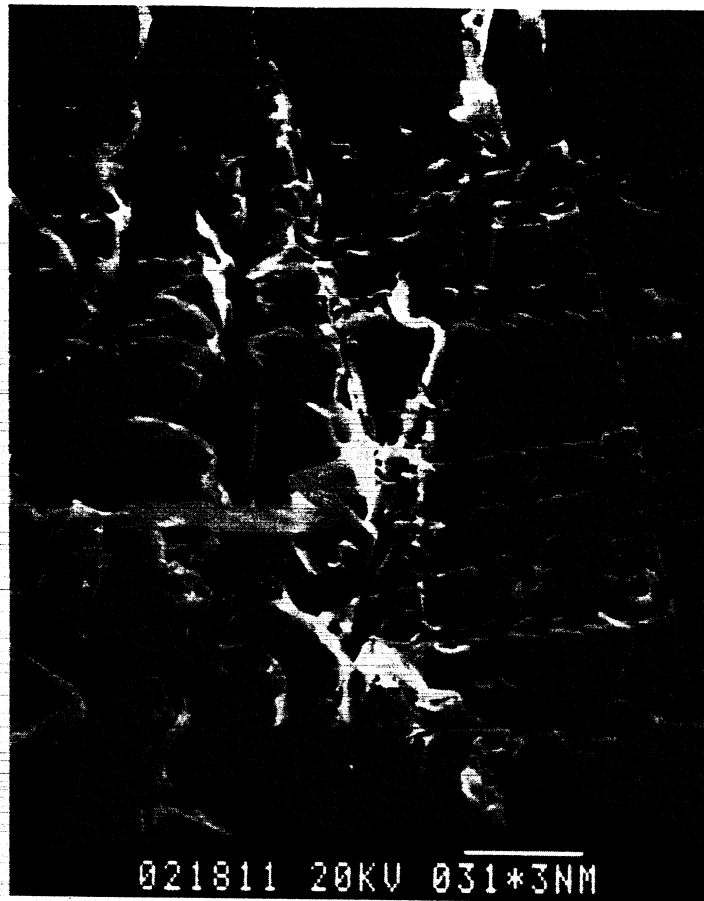


Figure 16. Scanning electron-micrograph of Teflon FEP roughened with 1000 grit SiC paper. Magnification $\times 500$.

Acknowledgements

We thank the National Science Foundation for support of M. K. Chaudhury, and the Industry/University Center for Biosurfaces at the State University of New York at Buffalo for the support of C. Yeung. This work constituted part of the Ph.D. thesis of Dr. Chaudhury (1986) and of the MS thesis of Mr. Yeung (1995).

REFERENCES

1. R. J. Good. *J. Am. Chem. Soc.* **74**, 5041 (1952).
2. R. J. Good, in: *Surface and Colloid Science*, Vol. 11, R. J. Good and R. R. Stromberg (Eds), pp. 1-29. Marcel Dekker, New York (1979).
3. R. J. Good. *J. Adhesion Sci. Technol.* **6**, 1269 (1992).
4. (a) R. N. Wenzel. *Ind. Eng. Chem.* **28**, 988 (1936);
(b) R. N. Wenzel. *J. Phys. Colloid Chem.* **53**, 1466 (1949).
5. R. J. Good and L. A. Girifalco. *J. Phys. Chem.* **64**, 561 (1960).

6. C. J. van Oss, M. K. Chaudhury and R. J. Good, *Separation Sci. Technol.* **22**, 1 (1987).
7. C. J. van Oss, M. K. Chaudhury and R. J. Good, *Chem. Rev.* **88**, 927 (1988).
8. R. J. Good, M. K. Chaudhury and C. J. van Oss, in: *Fundamentals of Adhesion*, L. H. Lee (Ed.), p. 153. Plenum Press, New York (1991).
9. H. W. Fox and W. A. Zisman, *J. Colloid Interface Sci.* **7**, 428 (1952).
10. (a) F. M. Fowkes, *Ind. Eng. Chem.* **56** (12), 40 (1964);
(b) F. M. Fowkes and M. A. Mostafa, *Ind. Eng. Chem. Prod. Res. Dev.* **17**, 3 (1980).
11. R. J. Good, *J. Colloid Interface Sci.* **59**, 398 (1977).
12. (a) R. E. Johnson, Jr. and R. H. Dettre, in: *Contact Angle, Wettability and Adhesion*, Adv. Chem. Ser. No. 43, 112. American Chemical Society, Washington, DC (1964);
(b) R. H. Dettre and R. E. Johnson, Jr., in: *Contact Angle, Wettability and Adhesion*, Adv. Chem. Ser. No. 43, p. 136. American Chemical Society, Washington, DC (1964).
13. W. A. Zisman, *Ind. Eng. Chem.* **53** (10), 18-38 (1963).